

7-2007

## Measurements of Mesospheric Sodium Abundance above the Hawaiian Islands

Lewis C. Roberts, Jr.  
*The Boeing Company*

L. William Bradford  
*The Boeing Company*

Christopher R. Neyman  
*W. M. Keck Observatory*

Alan Z. Liu  
*Embry Riddle Aeronautical University - Daytona Beach, liuz2@erau.edu*

Follow this and additional works at: <https://commons.erau.edu/db-physical-sciences>



Part of the [Physical Sciences and Mathematics Commons](#)

---

### Scholarly Commons Citation

Roberts, Jr., L. C., Bradford, L. W., Neyman, C. R., & Liu, A. Z. (2007). Measurements of Mesospheric Sodium Abundance above the Hawaiian Islands. *The Astronomical Society of the Pacific, 119*(). Retrieved from <https://commons.erau.edu/db-physical-sciences/10>

This Article is brought to you for free and open access by the College of Arts & Sciences at Scholarly Commons. It has been accepted for inclusion in Physical Sciences - Daytona Beach by an authorized administrator of Scholarly Commons. For more information, please contact [commons@erau.edu](mailto:commons@erau.edu).

# Measurements of Mesospheric Sodium Abundance above the Hawaiian Islands<sup>1</sup>

LEWIS C. ROBERTS, JR., AND L. WILLIAM BRADFORD

The Boeing Company, Kihei, HI; lewis.c.roberts@boeing.com, lawrence.w.bradford@boeing.com

CHRISTOPHER R. NEYMAN

W. M. Keck Observatory, Kamuela, HI; cneyman@keck.hawaii.edu

AND

ALAN Z. LIU

Department of Electrical and Computer Engineering, University of Illinois at Urbana-Champaign, Urbana, IL; liuzr@uiuc.edu

*Received 2007 April 4; accepted 2007 June 4; published 2007 July 3*

**ABSTRACT.** Laser guide stars have increased the utility of adaptive optics systems by expanding the number of observable objects. The most common type of laser excites sodium in the mesosphere, and mesospheric sodium density is key to the performance of the laser. While a variety of observatories have conducted studies of the mesospheric sodium density, there are no published studies from Hawaii, which is home to some of the largest telescopes in the world. This paper presents mesospheric sodium densities measured by the University of Illinois lidar for 165 hr spanning 25 nights over 3 years. The mean sodium column density is  $4.3 \times 10^9 \pm 0.2 \times 10^9 \text{ cm}^{-2}$ , with a seasonal peak in the winter, as found at many other sites. The variations in a given night can be as high as the seasonal variation. We predict the average photon returns for the 15 W Keck II laser and a proposed 50 W laser at the Advanced Electro-Optical System 3.6 m telescope for the observed sodium abundances.

## 1. INTRODUCTION

Laser guide stars (LGSs) have opened new avenues of research by allowing adaptive optics (AO) systems to observe a much wider range of targets than is possible with a natural guide star. One common type of LGS uses a laser beam centered at 589 nm to excite the mesospheric sodium layer (Thompson & Gardner 1987), which is deposited by the ablation of meteorites (Kane & Gardner 1993). The abundance of the sodium fluctuates seasonally, diurnally (States & Gardner 1999), and sporadically (Clemesha 1985). The density and variations of the sodium are also geographically dependent.

At times, the sodium layer can show enhancements in density of up to 10 times the average density. These sporadic layers are about 1 km in thickness and have lifetimes of a few hours. Their appearances and disappearances are very sudden, and their structure can change over time. Sporadic layers are rare at midlatitude sites, although they are fairly common over low-latitude sites, such as Hawaii. Sporadic layers over Hawaii have been studied by Kwon et al. (1988), Gardner et al. (1995), and Qian et al. (1998). The cause of the sporadic layers is still a matter of active research (Collins et al. 2002; Prasanth et al. 2006). Possible causes are tides, gravity waves, or photochem-

istry (Clemesha et al. 2002), and they are often linked to sporadic E-layers in the ionosphere. Sporadic layers are quite large: Qian et al. (1998) detected 18 sporadic events near Hawaii and measured their horizontal extents to be from 25 to 1560 km, with a mean of 440 km. This mean is biased downward by the short flight paths of the airborne lidar system. Using longer flight paths, Kane et al. (1991) found one sporadic layer as large as 1800 km.

The properties of the sodium layer above Hawaii have been studied in the past, although the measurements have been focused on understanding the layer itself, rather than its impact on sodium guide stars. Kwon et al. (1988) used a lidar system on Mauna Kea, while Gardner et al. (1995) used a lidar system on Haleakala, and the large-scale project Airborne Lidar and Observations of the Hawaiian Airglow (ALOHA) had campaigns in 1990 (Gardner 1991) and 1993 (Gardner 1995). None of these studies published significant column density statistics.

In Hawaii, Mauna Kea is the site of many of the foremost observatories in the world and is home to several existing sodium guide star systems. There is a 15 W laser at the Keck II Telescope (Wizinowich et al. 2006), a 4.5 W laser at the Subaru Telescope (Takami et al. 2006), and a 12 W laser at the Gemini Telescope (Boccas et al. 2006), and a 20 W solid-state laser is being developed for the Keck I telescopes (Hankla et al. 2006). Mauna Kea is also under consideration as the site of the Thirty Meter Telescope, which will have a laser guide star AO system (Joyce et al. 2006). The nearby Haleakala Observatory hosts

---

<sup>1</sup> Based on observations made at the Maui Space Surveillance System, operated by Detachment 15 of the US Air Force Research Laboratory's Directed Energy Directorate.

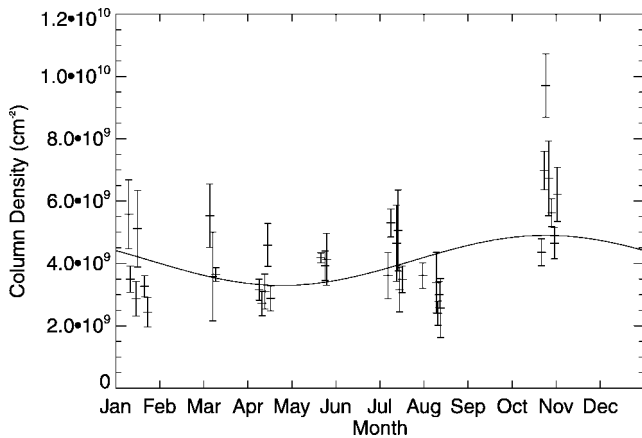


FIG. 1.—Median nightly sodium column density as a function of month of the year. The bars on each data point show the minimum and maximum sodium abundance measured on that night. A cosine fit to the data is overplotted, showing the seasonal variation in sodium density. The variations in sodium abundance on a given night can be as high as the seasonal variations.

the 3.6 m Advanced Electro-Optical System (AEOS) Telescope, which is considering acquiring a sodium guide star system.

This paper presents mesospheric sodium abundances gathered at the AEOS Telescope with a narrowband sodium-resonance lidar operated by the University of Illinois. While there have been no simultaneous observations from Haleakala and Mauna Kea, we expect the sodium abundance statistics to be valid at both sites. The size of the sporadic layers adds to our confidence in this assumption. A better understanding of the variation of sodium abundance can help plan observations and equipment upgrades at both Mauna Kea and Haleakala.

## 2. DATA COLLECTION

The sodium abundance data were collected as part of the Maui MALT (Mesosphere And Lower Thermosphere) program (Swenson 2005), which used a variety of instrumentation to study the upper atmosphere. The data presented here were collected using a sodium-laser lidar system set up in a coudé laboratory of the AEOS 3.6 m telescope (Chu et al. 2005). The laser was propagated up through the coudé optics, tertiary and secondary mirrors, and finally projected off of the primary mirror. The beam was focused 2.2 km above the telescope. From this point, it diverged and produced a 40 m diameter spot at a height of 100 km. The telescope primary collected any returning excited photons and reflected them back into the same coudé laboratory, where a receiver system recorded the signals. The lidar had a repetition rate of 50 Hz, with a laser pulse energy of 20–34 mJ.

The return signals are converted to sodium densities using the lidar equation (Gardner et al. 1986). The absolute sodium density is calibrated by the standard atmospheric density at 35 km, which is computed from the MSIS model (Mass Spectrometer and Incoherent Scatter; Hedin 1983, 1987, 1991). The

measured Rayleigh scatter from 35 km is then used to calibrate the mesospheric returns.

The raw return signal has a range resolution of 24 m. To improve the signal-to-noise ratio of the results, although at a cost of vertical resolution, 20 resolution cells are binned together, giving a resolution of 480 m. The processed data are then smoothed with 15 minute, 1 km full-width Hamming windows and are interpolated to 15 minute, 100 m resolution for easier analysis. The vertical smoothing does not remove much information, because the 1 km full-width Hamming window cuts off at approximately 500 m, close to the binned 480 m resolution. There is some smoothing effect in the temporal dimension, because the unsmoothed sodium density data have a temporal resolution of less than 2 minutes. Higher spatial resolution can be achieved at the cost of lowering the number of raw data points used and thus increasing the error bar on the density measurements.

Data were gathered in six observing runs, for a total of 25 nights of data (about 165 hr) between 2002 and 2005. During the observations, the lidar beam was pointed at zenith, to the north, to the east, back to zenith, to the south, and finally to the west. The directional beams had a zenith angle of 30°. The normal vertical resolution of the lidar is 480 m, but for non-zenith directions, this becomes 480 m multiplied by the cosine of the zenith angle. The nonzenith measurements are interpolated to the same height grid as that of the zenith measurements before all the measurements are interpolated onto the final grid spacing. The sequence was repeated throughout the night. The exceptions are the nights of 2002 January 9, April 9, July 14, and October 24. During these nights, the lidar was only pointed at zenith. This produced a higher temporal resolution data set, with a cadence of approximately 1.5 minutes.

## 3. ANALYSIS

### 3.1. Column Density

From the vertical profile of the sodium density, we computed the integrated column density by summing over the entire path. In Figure 1, we plot the median sodium column density for each night in the 4 yr data set as a function of month of the observation. The bars on each data point show the minimum and maximum column density for each night. The large range of values reflects the highly variable nature of the sodium layer. Some of the column density variability is due to the existence of sporadic layers, but even without a sporadic layer, the density changes throughout the night. The exact causes of this variation are still in considerable doubt (Clemesha et al. 2002). The intranight variations are also quite large.

We examined the diurnal variations and saw some weak correlations with time, but they were not statistically significant enough to warrant further analysis, although correlations have been detected at other sites (Gardner et al. 1986; Hu et al. 2003; Plane et al. 1999). We also analyzed the column density as a

function of year, and there was no obvious trend over the short baseline of observations we have.

To determine the seasonal dependency of the column density, we followed the analysis of Plane et al. (1999) and Hu et al. (2003) and fitted a cosine function to the column densities:

$$C_s = a \cos(2\pi[\tau - b]) + c, \quad (1)$$

where  $a$  is the amplitude of the variation,  $b$  is the time of maximum,  $c$  is the average column density, and  $C_s$  is the column density. We left out the semiamplitude terms, because there were insufficient data to fit those, and even in Plane et al. (1999), with its large amount of data, those terms are very small. Using a nonlinear least-squares fit yields values of  $1.1 \times 10^9 \pm 0.3 \times 10^9 \text{ cm}^{-2}$  for the amplitude,  $0.84 \pm 0.03$  for the time of maximum (November 2), and  $4.3 \times 10^9 \pm 0.2 \times 10^9 \text{ cm}^{-2}$  for the average. The reduced  $\chi^2$  value was 1.9, indicating that the fit was hampered by poor temporal coverage of the data. This fit is overplotted on Figure 1.

The seasonal variation has been measured at other sites. Plane et al. (1999) showed the seasonal variation from a data set combining 222 nights of data from Urbana, Illinois (latitude  $40^\circ$  north), and Fort Collins, Colorado (latitude  $41^\circ$  north). The combined data set had an amplitude of  $2.24 \times 10^9 \text{ cm}^{-2}$ , a time of maximum of 0.93 (December 4), and an average of  $4.26 \times 10^9 \text{ cm}^{-2}$ . The seasonal variation chart shown in Plane et al. (1999) has far more data points and shows that the inter-night variation can be as much as the seasonal dependency.

The seasonal variation of sodium was measured at the Starfire Optical Range (SOR) 3.5 m telescope (latitude  $35^\circ$  north) by Hu et al. (2003). From 1998 January to 2000 May, 46 nights of lidar data were collected using the same equipment that was used at AEOS. They fitted their data to the same seasonal variation equation used by Plane et al. (1999). The resulting fit had an amplitude of  $2.80 \times 10^9 \pm 0.37 \times 10^9 \text{ cm}^{-2}$ , a time of maximum of  $0.96 \pm 0.02$  (December 15), and an average of  $5.05 \pm 0.26 \times 10^9 \text{ cm}^{-2}$ .

Also working at SOR, Drummond et al. (2006) worked with data from the 50 W laser guide star mounted on the 3.5 m telescope. They were unable to come up with a direct estimate of the sodium abundance, but were able to determine the slope at the origin of the return flux as a function of laser power, which is directly related to the sodium abundance. They fitted a cosine to data from the laser returns and got a time of maximum of  $0.83 \pm 0.03$ . Since they were fitting to slope rather than to column density, we cannot directly compare the other two coefficients, but we can compare their ratios. Their ratio of amplitude to mean is 0.78, while our ratio is 0.26.

It has been known for decades that the sodium layer has a seasonal dependency, with a maximum in winter and a minimum in summer, and that this is a worldwide phenomenon (see Gardner et al. 1986 and references therein). Our results show the same seasonal trend, but the mean and amplitude are different. The average Hawaii sodium abundance is less than that

of more northern continental US sites, and the amplitude of variations is lower. Again, it should be kept in mind that the night-to-night and even intranight variations are larger than the seasonal variations.

### 3.2. Nightly Variation

As discussed in § 2, on four nights the sodium abundance data were measured approximately once every 1.5 minutes. These nights provide a detailed look at the vertical sodium abundance as a function of time. This is shown in Figure 2 for four nights in 2002: January 9, April 9, July 14, and October 24. The  $x$ -axis is time, the  $y$ -axis is altitude, and the intensity of the gray scale signifies the density of the sodium. Since the data were taken on a roughly, but not exact, 1.5 minute time cadence, the abundance measurements were interpolated onto a fixed time grid.

These plots illustrate that the structure of the sodium layer is highly chaotic and not easily predicted. The thickness of the layer varies along with the density. All four nights presented in Figure 2 show evidence of sporadic sodium layers. As the sporadic layers form, evolve, and eventually dissipate, the effective height of the sodium layer changes, causing a focus change on the wave-front sensor (WFS) observing the sodium guide star (O'Sullivan et al. 2000; Davis et al. 2006). The sporadic layers also display an increased density, with a corresponding increase in signal on the AO WFS. Along with this increased signal comes an increased variability of the WFS signal as the density fluctuates. It is important to remember that these sporadic layers are typically not seen at midlatitude sites, such as Lick Observatory, Palomar Observatory, or other US mainland observatories. Experiences at those observatories may not be applicable to Hawaii observatories, and vice versa.

## 4. LASER MODELING

We computed the sodium returns for the 15 W Keck II laser and the 50 W laser currently being used at the SOR 3.5 m telescope. In the case of the SOR laser, we simulated the return it would experience if it were located on the AEOS 3.6 m telescope. In both cases, these computations produce the number of photons at the entrance pupil of the telescope. The signal at the WFS is important to AO systems, and the total transmission loss has to be taken into account. In the case of AEOS, the AO system is located at the coudé focus, and the considerable number of optics in the system result in a transmission to the WFS of 0.3 (Roberts & Neyman 2002).

Milonni et al. (1998) derived an analytical model for the return from a pulsed laser exciting the mesospheric sodium layer. We used their equation (44) to compute the returns for

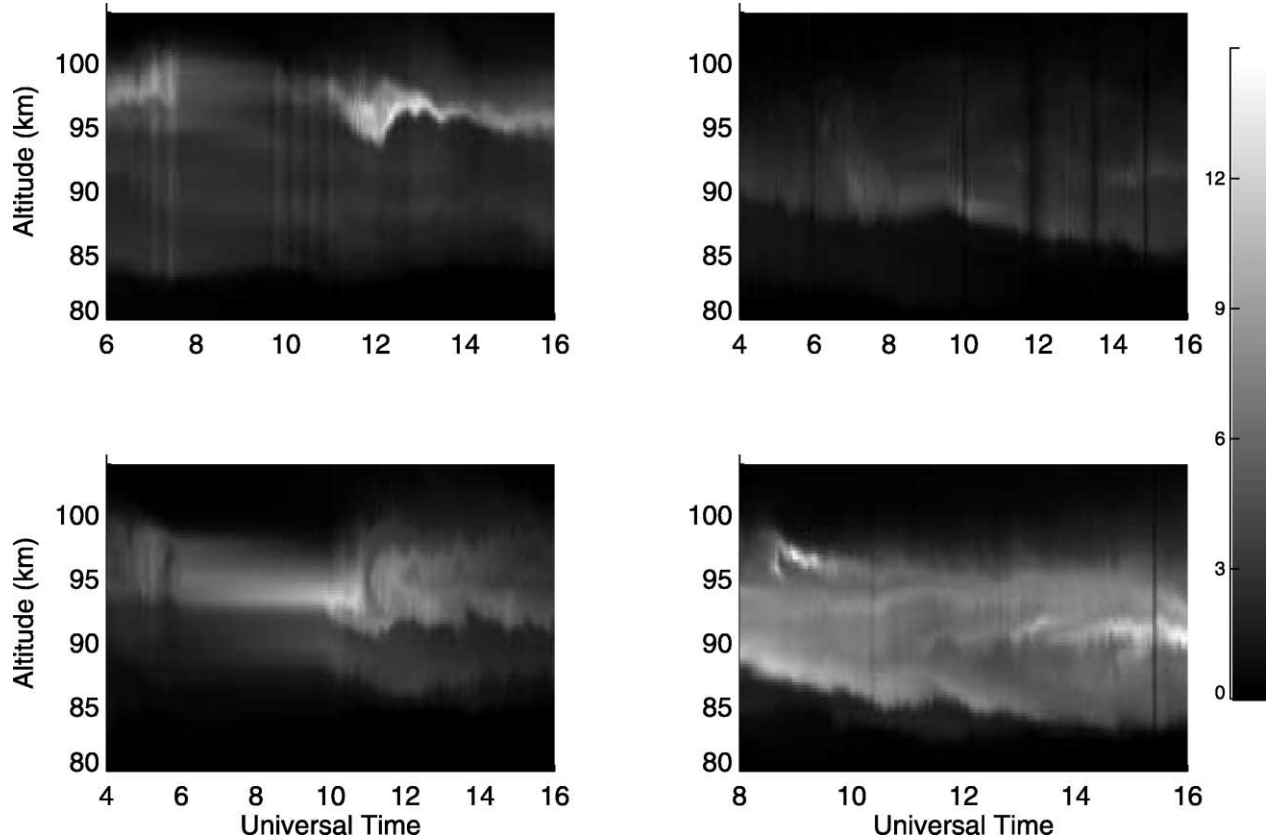


FIG. 2.—Sodium density as a function of time and altitude for four nights in 2002: January 9 (*top left*), April 9 (*top right*), July 14 (*bottom left*), and October 24 (*bottom right*). The label for the gray-scale bar is 1000 s of sodium atoms per  $\text{cm}^3$ .

the Keck II laser, which is a 15 W pulsed dye laser:

$$R_\gamma = \left( \frac{\pi}{4 \ln 2} \right) \frac{1}{8\pi} (A\tau_p + 1) \frac{T_0 C_s}{z^2} R_p a^2 \times \ln \left[ 1 + \left( \frac{4 \ln 2}{\pi} \right)^{3/2} \frac{T_0 P}{R_p I_{\text{sat}} a^2 \tau_p} \right] \quad (2)$$

(Wizinowich et al. 2006), where  $A$  is the decay rate,  $\tau_p$  is the FWHM duration of the laser pulse,  $T_0$  is the atmospheric transmission,  $C_s$  is the sodium column density,  $z$  is the height of the sodium layer,  $R_p$  is the pulse rate of the laser,  $a$  is the spot FWHM,  $P$  is the average laser power, and  $I_{\text{sat}}$  is the saturation intensity. This model assumes the pulse is spatially and temporally Gaussian. For atmospheric transmission, we used 0.9, a median value for the  $V$  band at Mauna Kea (Krisciunas et al. 1987). We used a decay rate of  $16 \text{ ns}^{-1}$ , a saturation of  $5 \text{ W cm}^{-2}$  (Milonni et al. 1998), a pulse length of 130 ns, a pulse rate of 26 kHz, a spot FWHM of 80 cm (Wizinowich et al. 2006), and an average on-sky power of 10 W. This average power was based on the logged power output of the laser and

also took into account the transmission of the beam director optics.

The photon flux ranges from 112 to  $490 \text{ photons cm}^{-2} \text{ s}^{-1}$ , with an average of  $176 \text{ photons cm}^{-2} \text{ s}^{-1}$  (9.2 mag). Wizinowich et al. (2006) report that there are normally  $55\text{--}140 \text{ photons cm}^{-2} \text{ s}^{-1}$  at the pupil of the telescope, which is slightly fainter than our results. There are several reasons for this. We do not know the sodium density during the Keck II runs, although on average the density should be close to the average densities reported in this paper. The atmospheric transmission is also unknown, but it should be close to the value above. The outgoing beam is probably not perfectly Gaussian; this will reduce the energy put into the spot at the sodium layer. Finally, the power output of the laser is known to fluctuate, and the value during the referenced observations was not reported.

We also model returns for the 50 W single-mode, continuous-wave laser currently being used at the SOR 3.5 m telescope (Telle et al. 2006). Milonni et al. (1999) followed up their earlier work on pulsed lasers with a model for continuous-wave lasers. For pulsed lasers, they included the effects of the geomagnetic field, the recoil of the sodium atoms on absorption and emission, and collisions of the sodium atoms with other species.

Pulsed lasers are more efficient at exciting the sodium atoms than the long-pulse laser that Keck II uses. We computed the return using equation (27) from Milonni et al. (1999):

$$R_{\gamma} = 3 \times 10^{-8} C_s T_o^2 P, \quad (3)$$

where  $P$  is in terms of watts, and  $C_s$  is in terms of atoms  $\text{cm}^{-2}$ . For an estimate of atmospheric extinction, we use the value for Mauna Kea as described above, but Haleakala should have a slightly higher extinction, due to the lower altitude of the observatory. This results in a photon flux ranging from 2000 to 13,000 photons, and an average returned photon flux of 5163 photons  $\text{cm}^{-2} \text{s}^{-1}$  (5.6 mag).

This result is for a circularly polarized laser beam under the assumption of no optical pumping in the sodium layer, so it represents a lower bound to the predicted photon flux. Complete optical pumping would result in a flux approximately 3 times larger (Milonni et al. 1999). Observations at SOR (Telle et al. 2006) show that some optical pumping occurs, so the expected photon flux should lie somewhere in between.

Using a laser guide star at the 3.5 m SOR Telescope in Albuquerque, New Mexico, Drummond et al. (2006) report that beacon returns are spatially varying. The beacon is brightest when parallel to the geomagnetic field, which at SOR is  $\sim 30^\circ$  south of zenith. This behavior is only found for beacons generated with circularly polarized light. Milonni et al. (1999) predicted that the geomagnetic field will cause a redistribution of the magnetic sublevel populations, reducing the degree of optical pumping. This will reduce the benefit that circularly polarized lasers have over linearly polarized lasers. In addition to the geomagnetic effects, Milonni et al. (1999) computes the impact of atomic collisions on the beacon brightness. They conclude that the effect of collisions will essentially eliminate the geomagnetic field effects. This does not appear to be the

case. Observations using circularly polarized continuous-wave lasers are needed in Hawaii and in other locations to further understand this behavior and to refine the theory.

## 5. CONCLUSIONS

We have derived the mesospheric sodium column densities above Haleakala, Maui, on 25 nights during 2002–2005. The average column density is  $4.3 \times 10^9 \text{ cm}^{-2}$ , with a seasonal variation of  $1.1 \times 10^9 \text{ cm}^{-2}$ , and with the peak in the late fall and the minimum in midspring. The times of minimum and maximum are similar to the results from other sites, although the seasonal amplitude is smaller. As is to be expected from a low-latitude site, we have found evidence of sporadic layers that have large variations in sodium column density and mean height. Inter- and intranight variations can be as large as the seasonal variations.

These measurements will assist in the design and operation of future sodium guide star systems in Hawaii. The minimum sodium density is a key driver for the output power requirements for the laser. We have used  $4.3 \times 10^9 \text{ cm}^{-2}$  as an average value, and  $2 \times 10^9 \text{ cm}^{-2}$  as the minimum value. It should be remembered that these results are specific to Hawaii and cannot easily be used to predict the sodium abundance at other sites. The sporadic layers commonly found in Hawaii are not often seen in midlatitude continental US sites, and the yearly mean changes with latitude.

The sodium abundance data were generously provided by the University of Illinois lidar group. The University of Illinois sodium lidar operation on Maui was supported by NSF grants ATM-00-03198 and ATM-03-38425. This research was funded by the Air Force Research Laboratory's Directed Energy Directorate, under contract FA9451-05-C-0257.

## REFERENCES

- Boccas, M., et al. 2006, Proc. SPIE, 6272, 62723L  
 Chu, X., Gardner, C. S., & Franke, S. J. 2005, J. Geophys. Res., 110, D09S03  
 Clemesha, B. R. 1985, J. Atmos. Terr. Phys., 57, 725  
 Clemesha, B. R., Batista, P. P., & Simonich, D. M. 2002, J. Atmos. Sol.-Terr. Phys., 64, 1321  
 Collins, S. C., et al. 2002, J. Atmos. Sol.-Terr. Phys., 64, 845  
 Davis, D. S., Hickson, P., Herriot, G., & She, C.-Y. 2006, Opt. Lett., 31, 3369  
 Drummond, J., Novotny, S., Denman, C., Hillman, P., Telle, J., & Moore, G. 2006, in Proc. 2006 AMOS Conf., 340  
 Gardner, C. S. 1991, Geophys. Res. Lett., 18, 1313  
 ———. 1995, Geophys. Res. Lett., 22, 2789  
 Gardner, C. S., Tao, X., & Papen, G. 1995, Geophys. Res. Lett., 22, 2809  
 Gardner, C. S., Voelz, D. G., Sechrist, C. F., Jr., & Segal, A. C. 1986, J. Geophys. Res., 91, 13659  
 Hankla, A. K., et al. 2006, Proc. SPIE, 6272, 62721G  
 Hedin, A. E. 1983, J. Geophys. Res., 88, 10170  
 ———. 1987, J. Geophys. Res., 92, 4649  
 Hedin, A. E. 1991, J. Geophys. Res., 96, 1159  
 Hu, X., Gardner, C. S., & Liu, A. Z. 2003, Chinese J. Geophys., 46, 432  
 Joyce, R., Boyer, C., Daggert, L., Ellerbroek, B., Hileman, E., Hunten, M., & Liang, M. 2006, Proc. SPIE, 6272, 62721H  
 Kane, T. J., & Gardner, C. S. 1993, Science, 259, 1297  
 Kane, T. J., Hostetler, C. A., & Gardner, C. S. 1991, Geophys. Res. Lett., 18, 1365  
 Krisciunas, K., et al. 1987, PASP, 99, 887  
 Kwon, K. H., Senft, D. C., & Gardner, C. S. 1988, J. Geophys. Res., 93, 14199  
 Milonni, P. W., Fearn, H., Telle, J. M., & Fugate, R. Q. 1999, J. Opt. Soc. Am. A, 16, 2555  
 Milonni, P. W., Fugate, R. Q., & Telle, J. M. 1998, J. Opt. Soc. Am. A, 15, 217  
 O'Sullivan, C., et al. 2000, Exp. Astron., 10, 147  
 Plane, J. M. C., Gardner, C. S., Yu, J., She, C. Y., Garcia, R. R., & Pumphrey, H. C. 1999, J. Geophys. Res., 104, 3773  
 Prasanth, P. V., Kumar, Y. B., & Rao, D. N. 2006, Proc. SPIE, 6409, 64090S

Qian, J., Gu, Y., & Gardner, C. S. 1998, *J. Geophys. Res.*, 103, 6333  
Roberts, L. C., Jr., & Neyman, C. R. 2002, *PASP*, 114, 1260  
States, R. J., & Gardner, C. S. 1999, *J. Geophys. Res.*, 104, 11783  
Swenson, G. R. 2005, *J. Geophys. Res.*, 110, D09S01  
Takami, H., et al. 2006, *Proc. SPIE*, 6272, 62720C

Telle, J., Drummond, J., Denman, C., Hillman, P., Moore, G., Novotny, S., & Fugate, R. 2006, *Proc. SPIE*, 6215, 62150K  
Thompson, L. A., & Gardner, C. S. 1987, *Nature*, 328, 229  
Wizinowich, P. L., et al. 2006, *PASP*, 118, 297